

Mitochondrial Outer Membrane Proteome of *Trypanosoma brucei* Reveals Novel Factors Required to Maintain Mitochondrial Morphology*

Moritz Niemann‡§, Sebastian Wiese¶||, Jan Mani‡, Astrid Chanfon‡, Christopher Jackson||, Chris Meisinger‡**, Bettina Warscheid¶‡‡, and André Schneider‡‡‡

Trypanosoma brucei is a unicellular parasite that causes devastating diseases in humans and animals. It diverged from most other eukaryotes very early in evolution and, as a consequence, has an unusual mitochondrial biology. Moreover, mitochondrial functions and morphology are highly regulated throughout the life cycle of the parasite. The outer mitochondrial membrane defines the boundary of the organelle. Its properties are therefore key for understanding how the cytosol and mitochondria communicate and how the organelle is integrated into the metabolism of the whole cell. We have purified the mitochondrial outer membrane of *T. brucei* and characterized its proteome using label-free quantitative mass spectrometry for protein abundance profiling in combination with statistical analysis. Our results show that the trypanosomal outer membrane proteome consists of 82 proteins, two-thirds of which have never been associated with mitochondria before. 40 proteins share homology with proteins of known functions. The function of 42 proteins, 33 of which are specific to trypanosomatids, remains unknown. 11 proteins are essential for the disease-causing bloodstream form of *T. brucei* and therefore may be exploited as novel drug targets. A comparison with the outer membrane proteome of yeast defines a set of 17 common proteins that are likely present in the mitochondrial outer membrane of all eukaryotes. Known factors involved in the regulation of mitochondrial morphology are virtually absent in *T. brucei*. Interestingly, RNAi-mediated ablation of three outer membrane proteins of unknown function resulted in a collapse of the network-like mitochondrion

of procyclic cells and for the first time identified factors that control mitochondrial shape in *T. brucei*. *Molecular & Cellular Proteomics* 12: 10.1074/mcp.M112.023093, 515–528, 2013.

Trypanosomatids are unicellular parasites that cause devastating diseases in both humans and animals. They include *Trypanosoma brucei*, two subspecies of which cause human sleeping sickness, and *Trypanosoma cruzi* and *Leishmania* spp., which are responsible for Chagas disease and leishmaniasis, respectively. The treatment of these diseases is still unsatisfactory, and new drugs are urgently needed (1).

In addition to their clinical importance, some trypanosomatids are highly accessible experimental model systems for investigating general biological processes. Moreover, trypanosomatids appear to have diverged from all other eukaryotes very early in evolution and therefore show many unique features, some of which might reflect primitive traits that were present in the universal ancestor of all eukaryotes (2).

Many of these features concern the mitochondrion. Its genome consists of two genetic elements, maxi- and minicircles, which are highly topologically interlocked and localized to a discrete region within the organelle (3). Many mitochondrial genes represent cryptogenes whose primary transcripts have to be processed via extensive RNA editing in order for them to become functional mRNAs (4). The mitochondrial genome lacks tRNA genes, indicating that trypanosomatids, unlike most other eukaryotes, import all mitochondrial tRNAs from the cytosol (5). The mitochondrial outer membrane (OM)¹ of trypanosomatids has an unusual protein translocase, termed ATOM (6), that is similar to the canonical protein import pore

From the ‡Department of Chemistry and Biochemistry, University of Bern, CH-3012 Bern, Switzerland; ¶Faculty of Biology and BIOS Centre for Biological Signalling Studies, University of Freiburg, 79104 Freiburg, Germany; ||Division of Human Genetics, Department of Paediatrics and Department of Clinical Research, Inselspital, University of Bern, CH-3012 Bern, Switzerland; **Institut für Biochemie und Molekularbiologie, ZBMZ and BIOS Centre for Biological Signalling Studies, Universität Freiburg, 79104 Freiburg, Germany

Received August 14, 2012, and in revised form, November 14, 2012
Published, MCP Papers in Press, December 6, 2012, DOI 10.1074/mcp.M112.023093

¹ The abbreviations used are: ATOM, archaic translocase of the mitochondrial outer membrane; ER, endoplasmic reticulum; IM, inner membrane; MS, mass spectrometry; OM, outer membrane; POMP, present in the outer mitochondrial membrane proteome; VDAC, voltage-dependent anion channel.

Tom40 (7), as well as to the bacterial Omp85-like protein family that is involved in protein translocation (6, 8, 9).

Trypanosomatids, unlike most other eukaryotes, have a single continuous mitochondrion throughout their life and cell cycle (10, 11). Its morphology changes from a complex network in procyclic cells to a single tube-like structure in the bloodstream form (12). Nothing is currently known about how the different morphologies of the mitochondrion are established and maintained. The changes in organellar shape correlate with large functional differences between the procyclic mitochondrion and the bloodstream form. Only organelles of the procyclic stage are capable of oxidative phosphorylation, whereas in the bloodstream form, energy is produced by means of substrate-level phosphorylation (13–15).

Recently, a proteomic study of the whole *T. brucei* mitochondrion detected 401, 196, and 283 proteins that could be assigned to mitochondria with high, medium, and low confidence, respectively (16). A follow-up study analyzed mitochondrial membrane fractions and identified 202 proteins that contained one or more predicted transmembrane helices and were associated with mitochondria with various levels of confidence (17). This added 65 new proteins to the previously defined mitochondrial proteome. Moreover, the proteomes of the respiratory complexes (18) and the mitochondrial ribosomes (19) also have been characterized. However, an inventory of the mitochondrial OM is still lacking. In fact, the way the mitochondria were isolated in the studies described above suggests that they are depleted of OM proteins (20).

The OM separates the organelle from the cytosol. Detailed knowledge about the OM proteome is therefore a prerequisite for a comprehensive understanding of how the cytosol and mitochondria communicate and how the organelle is integrated into the metabolism of its host cell. The OM is the first barrier-imported protein that tRNAs face while they are being transported into the mitochondrion. Knowing its proteome will therefore also help us understand the molecular mechanisms of these two processes.

Presently, only four mitochondrial OM proteins are known in trypanosomatids. These are the voltage-dependent anion channel (VDAC) that serves as a metabolite transporter (21) and three components of the mitochondrial protein import system. The latter are the trypanosomal SAM50 orthologue, which mediates the insertion of beta-barrel proteins into the OM (22); ATOM, the general mitochondrial preprotein translocase (6); and pATOM36, which may serve as a receptor for a subset of imported proteins (23). The situation is only marginally better outside the trypanosomatids, and the only global proteomic analyses of the mitochondrial OM that have been performed are of the two fungal species *Saccharomyces cerevisiae* (24) and *Neurospora crassa* (25) and the plant *Arabidopsis thaliana* (26). These studies detected 82 and 30 resident OM proteins, respectively, in the fungal species and 42 proteins in the plant.

Here we present a comprehensive proteomic analysis of the mitochondrial OM of the procyclic form of *T. brucei*. To that end, we established a purification procedure allowing the isolation of a highly enriched OM fraction. To identify *bona fide* OM proteins, we employed label-free quantitative mass spectrometry to establish abundance profiles of several hundred proteins across four and six subcellular fractions including highly purified OMs. This allowed us to identify 82 proteins that could be localized to the mitochondrial OM with high confidence. The ablation of three trypanosomatid-specific proteins of unknown function affects mitochondrial morphology and thus defines the first factors controlling mitochondrial morphology in *T. brucei*. Based on a recent global RNAi study (27), nine OM proteins are essential for normal growth under all tested conditions, including in the disease-causing bloodstream form of the parasite, indicating that they could be novel potential drug targets.

EXPERIMENTAL PROCEDURES

Cell Culture—Both procyclic wild-type *T. brucei* strain 427 and transgenic *T. brucei* strain 29–13 were used in this study. All cell lines were grown in SDM-79, which was supplemented with 5% (427) or 10% (29–13) fetal calf serum (Sigma). For OM purification, cells were harvested at late log phase corresponding to a density of 3.0×10^7 to 4.0×10^7 cells/ml.

Purification of the Mitochondrial OM of *T. brucei*—Cells were lysed under isotonic conditions via N_2 cavitation (28). Mitochondrial vesicles were isolated by means of differential centrifugation and subsequent Nycodenz step gradients as described elsewhere (20). Mitochondrial vesicles were used as a starting point to prepare a highly enriched mitochondrial OM fraction using a modified version of the procedure described in Refs. 29 and 30 (see Fig. 1A for an overview). 100 mg of mitochondrial vesicles, isolated from 4×10^{11} to 5×10^{11} cells, were diluted to 10 mg/ml in swelling buffer consisting of 5 mM potassium phosphate, pH 7.2, containing 5 mM EDTA and 1 mM PMSF. The vesicles were kept under hypotonic conditions for 25 min on ice and allowed to swell. Subsequently, they were homogenized with 20 strokes using a Dounce homogenizer (Wheaton, Millville, NJ) with a loose-fitting Teflon pestle to dislodge the OM from the inner membrane (IM). In order to separate IM vesicles and residual mitochondria from the lower density OM, the mixture was loaded on top of a 0/15/32/60% (w/v) sucrose step gradient containing buffer A (10 mM MOPS, KOH pH 7.2, and 2.5 mM EDTA). Centrifugation was done for 1 h at 2 °C at 100,000g, and both the bottom fraction (32/60% sucrose interface) corresponding to the IM and the top fraction (15/32% sucrose interface) corresponding to crude OM were collected. The latter was adjusted to 50% (w/v) sucrose in buffer A and overlaid with two layers consisting of an equal volume of buffer A containing 32% (w/v) sucrose and one of buffer A lacking sucrose. The flotation gradient was centrifuged for 5 h at 2 °C at 240,000g, and the fraction at the 0/32% sucrose interphase corresponding to pure OM was collected. Approximately 300 μ g OM per 100 mg mitochondrial vesicles was obtained.

A crude endoplasmic reticulum (ER) fraction was prepared using the supernatant resulting from centrifugation after the isotonic N_2 -cavitation of the cells (20, 28). This supernatant was subjected to a clearing spin for 30 min at 4 °C and 30,000g in order to remove remaining mitochondrial vesicles and cell debris. From this cleared supernatant, the crude ER fraction was harvested via ultracentrifugation (2 h at 4 °C and 100,000g).

Sample Preparation for Proteomic Analysis—Proteins from organellar fractions were precipitated using 10% trichloroacetic acid or 4:1 (v/v) methanol (MeOH)/chloroform (31). Protein pellets were obtained via centrifugation for 20 min at 4 °C and 21,100g and were redissolved in 60% MeOH/20 mM NH₄HCO₃ (pH 7.8). Tryptic digestion of proteins was performed overnight at 37 °C, and the resulting peptides were dried *in vacuo* and redissolved in 15 μl 0.1% trifluoroacetic acid.

Mass Spectrometry—Ultra-high-pressure LC separations were conducted on the UltiMate 3000 RSLCnano HPLC system (Thermo Scientific, Idstein, Germany). Peptides were concentrated and washed on a C18 μ-pre-column (Acclaim® PepMap μ-Pre-column Cartridge; 0.3 mm × 5 mm, particle size 5 μm, Thermo Scientific) for 10 min with 0.1% trifluoroacetic acid at a flow rate of 30 μl/min, and they were subsequently separated on a 25 cm × 70 μm C18-column (Acclaim PepMap RSLC column, 2 μm particle size, 100 Å pore size, Thermo Scientific) at a flow rate of 300 nl/min with a linear gradient consisting of 4%–26% solvent B (0.1% (v/v) trifluoroacetic acid in 84% (v/v) acetonitrile) over 140 min and 26%–43% solvent B over 10 min. Eluting peptides were directly analyzed via tandem mass spectrometry (MS/MS) on an LTQ-Orbitrap XL instrument (Thermo Scientific, Bremen, Germany) equipped with a nanoelectrospray ion source. A spray voltage of 1.5 kV and an ion transfer tube temperature of 200 °C were applied. The instrument was calibrated using standard compounds and operated in the data-dependent mode. Survey mass spectrometry (MS) spectra from *m/z* 370–1700 were acquired in the orbitrap at a resolution of 60,000 at *m/z* 400 with an automatic gain control value of 5 × 10⁵ ions and a maximum fill time of 500 ms. A TOP5 method was applied. The five most intense multiple charged peptides were sequentially subjected to low-energy collision-induced dissociation experiments in the linear ion trap, applying a target accumulation value of 10,000 with a maximum fill time of 400 ms, a normalized collision energy of 35%, an activation *q* of 0.25, and an activation time of 30 ms. A dynamic exclusion time of 45 s with a parent mass accuracy of 20 ppm was applied.

Data Analysis—Mass spectrometric data from two independent experiments were processed separately using the software MaxQuant (version 1.2.0.18) (32, 33). For protein identification, spectra were correlated with the *Trypanosoma brucei* protein database (TriTrypDB, version 3.1), containing 9826 protein entries, using Andromeda (33). All searches were performed with tryptic specificity allowing up to two missed cleavages. Oxidation of methionine and acetylation of protein N termini were considered as variable modifications. No fixed modifications were considered. Raw data were recalibrated using the “first search” option of Andromeda with the full database employing a mass error of 20 ppm for precursor ions and 0.5 Da for fragment ions. Mass spectra were searched using the default settings of Andromeda. The mass tolerance values for precursor and fragment ions were 6 ppm and 0.5 Da, respectively. A false discovery rate of 1% was applied to both the peptide and the protein level. For retrieving information about protein abundance, the label-free protein quantification option in MaxQuant was enabled using default settings and the “match between runs” option with a retention time window of 2 min. Only razor and unique peptides were considered for quantification. Protein intensity values were normalized to the total ion current of the pure mitochondria and the OM/ER fraction of experiments 1 and 2, respectively. To establish protein profiles, the intensity values of a given protein were plotted against the different subcellular fractions and normalized to one. For statistical analysis, protein abundance profiles were hierarchically clustered using Euclidean distances and complete linkage in the R software environment. Only proteins identified and quantified in both datasets were considered for clustering analysis; mass spectra of single peptide identifications are shown in supplemental Fig. S1. For the calculation of log₁₀ intensity plots, intensity values were normalized to the intensity

value of HSP60 (Tb927.10.6400), representing the most abundant protein in the pure mitochondrial fraction. The mean of the normalized intensity values of each protein was then calculated and multiplied by the intensity of HSP60 in experiment 2.

Proteinase K Digestion—Mitochondrial vesicles (20) (25 μg each) were resuspended in 20 mM Tris, pH 7.2, 15 mM KH₂PO₄, 20 mM MgSO₄ and 0.6 M sorbitol in a total volume of 50 μl. Proteinase K treatment (Roche Applied Science; final concentration of 50 or 250 μg/ml) was done for 15 min on ice. The reactions were stopped by adding PMSF to a final concentration of 5 mM. Subsequently, mitochondrial vesicles were sedimented for 3 min at 4 °C and 6800g in a tabletop centrifuge, and the resulting pellet was resuspended in SDS sample buffer containing 60 mM β-mercaptoethanol and boiled for 3 min at 95 °C.

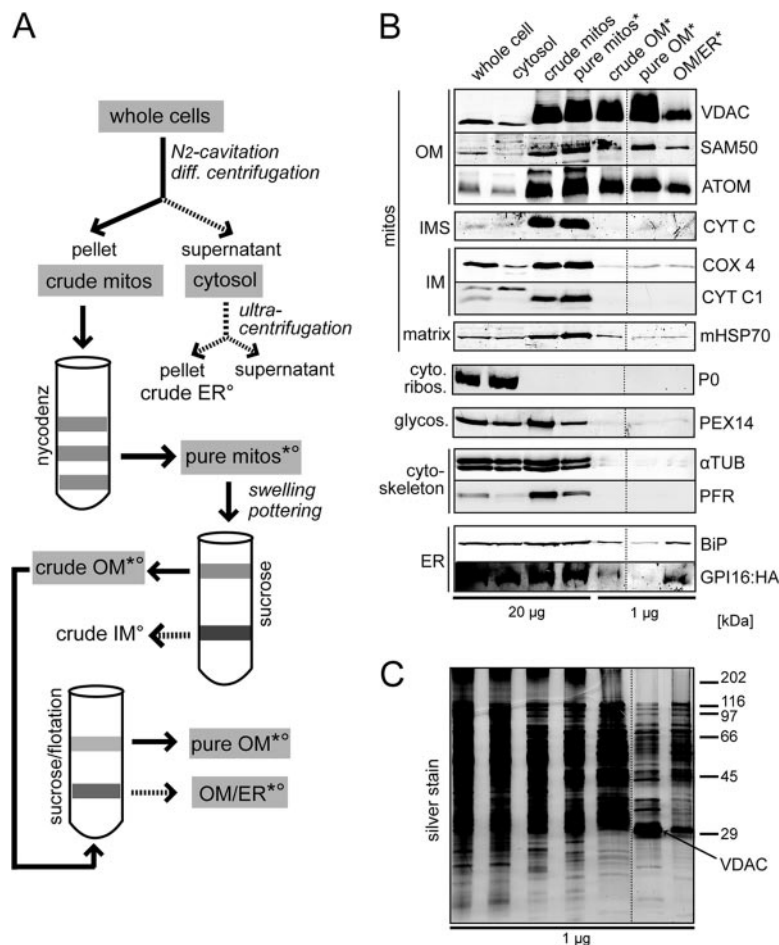
Miscellaneous—Protein concentrations were determined using BCA protein assay reagent (Pierce). Protein samples were analyzed via conventional SDS-PAGE and immunoblotting using the Odyssey Clx infrared imaging system (LI-COR Biosciences, Lincoln, NE). Proteins were C-terminally c-MYC-tagged; SAM35 was C-terminally tagged with the HA-epitope using a pLew100-based construct (34, 35). Inducible RNAi cell lines of POMP9, -14, and -40 were prepared using pLew100-based stem-loop constructs (35, 36). As inserts, we used a 428-bp fragment (nucleotides 686–1113) of POMP9, a 360-bp fragment (nucleotides 1–360) of POMP14, and a 303-bp fragment (nucleotides 12–314) of POMP40. Immunofluorescence of paraformaldehyde-fixed cells was done as described elsewhere (37).

RESULTS AND DISCUSSION

Purification of the Mitochondrial OM from *T. brucei*—The mitochondrial OM purification strategy for *T. brucei* was adapted from protocols for yeast (29, 30) and is outlined in Fig. 1A. In the first step, procyclic *T. brucei* cells are lysed under isotonic conditions using N₂ cavitation (28). After DNA digestion and differential centrifugation, a crude mitochondrial fraction (crude mitos) is obtained and further purified via Nycodenz gradient sedimentation, yielding pure mitochondria (pure mitos), which have an intact OM (20). This fraction is subjected to a swelling step under hypotonic conditions and extensively homogenized. The aim of this step is to disrupt the OM and dislodge it from the IM. The resulting homogenate is resolved on a sucrose gradient yielding two main fractions. The denser, more abundant one is enriched for IM markers, whereas the less dense, minor fraction corresponds to crude OM. The latter is collected and subjected to a sucrose flotation gradient, again resulting in two fractions, one consisting of pure OM and the other of both ER and OM (OM/ER). From 4 × 10¹¹ cells, ~300 μg of pure OM fraction was obtained.

Selected fractions of the purification (Fig. 1A, gray boxes) were analyzed using silver staining (Fig. 1C) and on immunoblots using a panel of antisera directed against marker proteins for submitochondrial and different subcellular compartments (Fig. 1B). The results show that the previously characterized trypanosomal OM proteins, VDAC (21), SAM50 (22), and ATOM (6), are strongly enriched in the pure OM fraction. A quantification of the immunoblots indicates that the enrichment factors for the three proteins between whole cells and the pure OM fraction are between 50- and 60-fold (it should be noted that the three last lanes of the immunoblots

FIG. 1. Purification of mitochondrial OM of *T. brucei*. *A*, outline of the OM purification scheme. The fractions that were analyzed in the immunoblot in *B* are highlighted by gray boxes. The fractions of the first and second independent OM purifications that were analyzed via mass spectrometry are denoted by * and °, respectively. *B*, 20 μ g and 1 μ g of the indicated fractions were analyzed on immunoblots using antisera directed against the indicated marker proteins of the subcellular compartments depicted on the left. Antisera directed against the following proteins were used: COX 4, cytochrome oxidase subunit 4; CYT C1, cytochrome C1; P0, ribosomal stalk protein P0; PEX14, glycosomal membrane protein PEX14; α TUB, α -tubulin; PFR, paraflagellar rod proteins; BiP, ER-localized Hsp70-like chaperone. The dotted line indicates that a lane was removed electronically between the “crude OM” and “pure OM” fractions. *C*, silver stain of a gel containing the same fractions as were analyzed on the immunoblot in *B*.



in Fig. 1*B* contain 20-fold less protein than all other lanes). Markers for the intermembrane space, the IM, and the matrix are strongly depleted in the pure OM fraction, indicating that there is only very little contamination by components from the other mitochondrial subcompartments. Moreover, the pure OM fraction is essentially free of cytosol, glycosomes, and components of the cytoskeleton. In the case of the ER, both BiP, a component of the ER lumen, and a tagged transmembrane subunit of the trypanosomal glycosylphosphatidylinositol transamidase complex (GPI16:HA) (38) were analyzed. Both ER proteins are depleted in the pure OM fraction, but to a lesser extent than the markers for the other subcellular compartments. Interestingly, the most dense fraction recovered from the sucrose flotation gradient, termed OM/ER, is enriched for OM as well as for both ER markers.

Finally, the pure OM fraction was also subjected to electron microscopy using uranyl acetate for negative staining. This analysis revealed a population of single membrane-bounded vesicles of similar morphology but different diameters, consistent with a highly enriched mitochondrial OM fraction (supplemental Fig. S2) (39).

Mass Spectrometric Analysis of Subcellular Fractions—A eukaryotic cell contains many different membranes, of which

the mitochondrial OM is of minor abundance. Moreover, the OM is known to be tightly associated with the IM and to interact with parts of the ER (40). This makes it difficult, if not impossible, to prepare OM that is free of contaminants, the most likely sources of which are the IM and the ER. In order to identify *bona fide* OM proteins and distinguish them from contaminants, we employed protein abundance profiling via high-resolution MS (41–43). Two independent experiments were performed to characterize the mitochondrial OM proteome. In the first, crude and pure OM fractions, as well as pure mitos and OM/ER fractions, were analyzed (Fig. 1*A*; look for asterisks). In the second experiment, the analysis was extended by including the crude ER and crude IM fractions (Fig. 1*A*; see “°”). All fractions were analyzed via high resolution LC/MS to provide a comprehensive dataset for label-free quantitative protein profiling. Table I provides a summary of the number of MS/MS spectra acquired, as well as the number of peptides and proteins identified in individual fractions (supplemental Tables S1A–S1D and S2A–S2D). Altogether, more than 100,000 MS/MS spectra were acquired, resulting in the identification of 2142 unique proteins with a false discovery rate of $\leq 1\%$. In experiment 2, the inclusion of the crude ER and crude IM fractions led to the identification of an

TABLE I

Overview of MS/MS data and protein identification numbers obtained via proteomic analysis of distinct subcellular fractions from two independent OM purification experiments

	Experiment 1						Experiment 2						
	Total (1 + 2)	Total	Pure mitos	Crude OM	Pure OM	OM/ER	Total	Crude ER	Pure mitos	Crude IM	Crude OM	Pure OM	OM/ER
MS/MS spectra	117,450	36,035	11,547	8331	8304	7853	81,415	13,054	14,238	13,045	13,751	11,768	15,558
Identified spectra	45,013	14,430	6,128	2932	2691	2679	30,583	4761	5467	4828	5042	4132	6353
Identified proteins	2142	1309	1094	711	609	689	1896	1169	1046	1006	984	688	1122

additional 587 proteins that were not found in experiment 1. Protein identification numbers obtained for the pure mitos and pure OM fraction from the two independent experiments were highly consistent, with variations of 4% and 11%, respectively. Moreover, the corresponding overlaps of proteins identified in these fractions were 67.6% and 59.1%, underscoring the high consistency of our data.

Localization of Proteins by Correlation of Abundance Profiles—To further distinguish between OM constituents and co-purified contaminants, we relied on quantitative feature analysis in MS survey scans using the MaxQuant algorithm (32, 33). This allowed us to determine the intensity values of all proteins identified in the four and six different subcellular fractions obtained during the two OM purifications.

Altogether, 1062 proteins were quantitatively followed through both experiments (supplemental Table S3), and the corresponding normalized abundance profiles were calculated. Fig. 2 depicts the abundance profiles of marker proteins of the mitochondrial OM (VDAC, SAM50, and ATOM) and IM (COX 4 and CYT C1), as well as those of the ER (BiP and GPI16). Notably, MS-based protein abundance profiles of subcellular and suborganellar marker proteins were highly reproducible between the two independent experiments (Fig. 2) and essentially congruent with the ones obtained via immunoblotting (Fig. 1B). OM proteins characteristically exhibited low intensities in crude ER, pure mitos, and IM fractions but showed a distinct maximum in pure OM fractions. Notably, the measured relative intensity of OM proteins typically increased by more than 2-fold between crude and pure OM fractions, thereby facilitating the reliable identification of even minor OM constituents. Contaminants of the OM mainly derived from the ER and the IM (Fig. 1B). Such components could be well distinguished from the OM proteome based on their abundance profiles exhibiting distinct maxima in either the crude ER or the crude IM fraction, as exemplarily shown for the marker proteins GPI16, BiP, COX 4, and CYT C1 (Fig. 2).

Through this statistical approach, a cluster of 83 putative OM proteins was obtained. However, because it contained the IM-localized ADP/ATP carrier, which is the most abundant mitochondrial membrane protein and therefore the most obvious contaminant of the pure OM fraction, this protein was excluded from the cluster, resulting in an OM proteome of 82 proteins (Fig. 3A, supplemental Table S3). All cluster components are listed in Tables II and III, including information about

their accession number, name, predicted protein domains, molecular weight, and number of putative transmembrane domains. They comprise all four previously known mitochondrial OM proteins: VDAC (21), SAM50 (22), ATOM (6), and pATOM36 (23). Using BLAST, we found 38 proteins of the OM cluster that showed similarities to proteins of known function in other eukaryotes and two trypanosomatid-specific components of the OM protein import system (6, 23). The function of 42 proteins (51% of the OM proteome) is unknown. These proteins were termed POMP (present in the outer mitochondrial membrane proteome) and numbered. 16 POMP have known protein domains (Table II), and 33 proteins (40% of the total proteome) are conserved in trypanosomatids only (Table II, asterisks).

The power of the protein abundance profiling approach is illustrated by the fact that, except for the ADP/ATP carrier mentioned above, the OM proteome lacks all the common contaminants, such as the highly abundant ribosomal proteins, eukaryotic translation elongation factor 1a, and tubulins. The same applies to proteins known to reside in other submitochondrial compartments.

Interestingly, MICU1 (44), the regulatory partner of the recently characterized mitochondrial calcium uniporter (MCU) (45, 46), was also found in the OM cluster. MICU1 is a peripheral membrane protein that interacts with the IM protein MCU. Our results suggest the exciting possibility that MICU1, unlike what was assumed before, might not be localized in the IM and, together with MCU, might form contact sites between the two mitochondrial membranes.

It should be considered in this context that our OM cluster might also contain dually localized OM proteins, as long as their second localization is outside the mitochondria.

Even though it was not the aim of our study, it is worth noting that our quantitative proteomics survey further allows us to define a second cluster of 282 proteins that constitutes the mitochondrial IM proteome (Fig. 3A). Its components showed the highest enrichment in the crude IM fraction and significant but lower intensity values in the pure mitochondrial fraction (see Fig. 2, experiment 2). Interestingly, 37% of these proteins are not found in the least stringent list of IM proteins that has been published before (17).

To demonstrate the consistency of the data obtained from both experiments, the median and the middle 50% of the profiles of all the 82 and 282 proteins present in the OM and IM clusters are depicted in Figs. 3B and 3C, respectively.

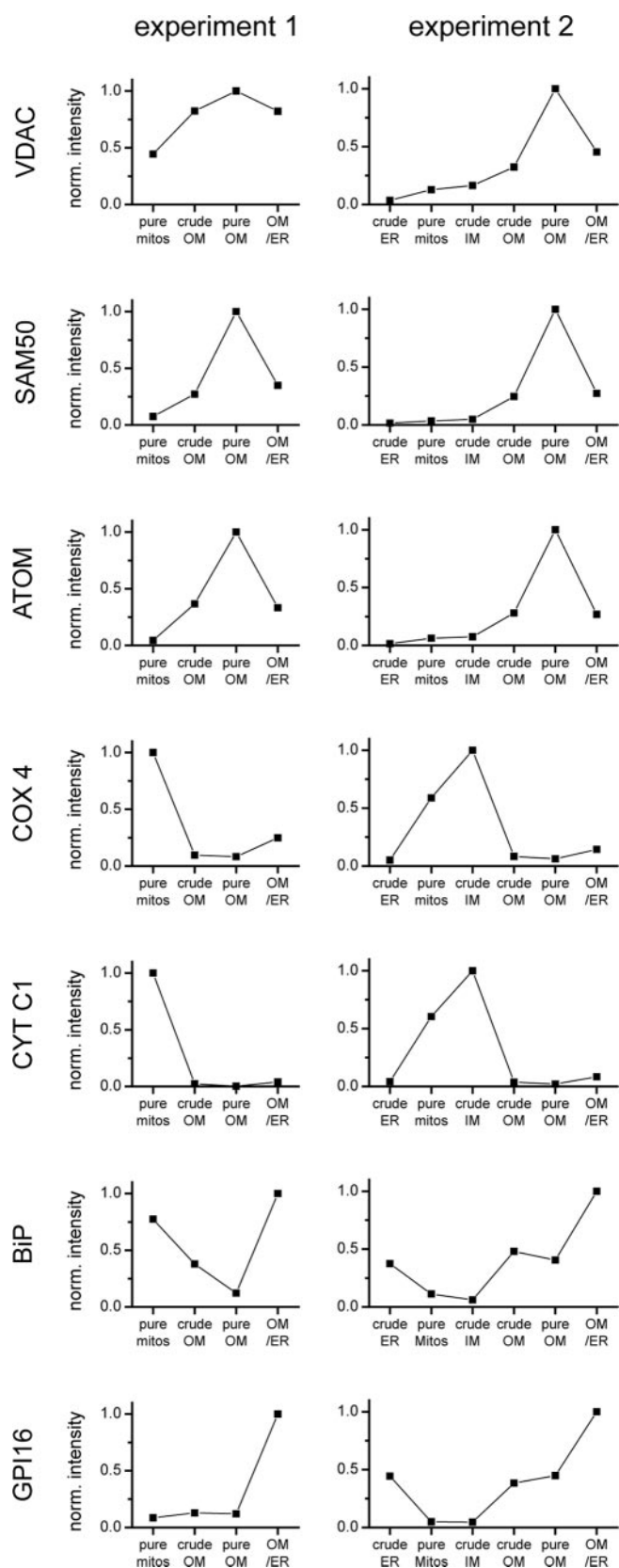


FIG. 2. **Abundance profiles of marker proteins.** The intensities of selected marker proteins of the OM (VDAC, SAM50, ATOM), the IM

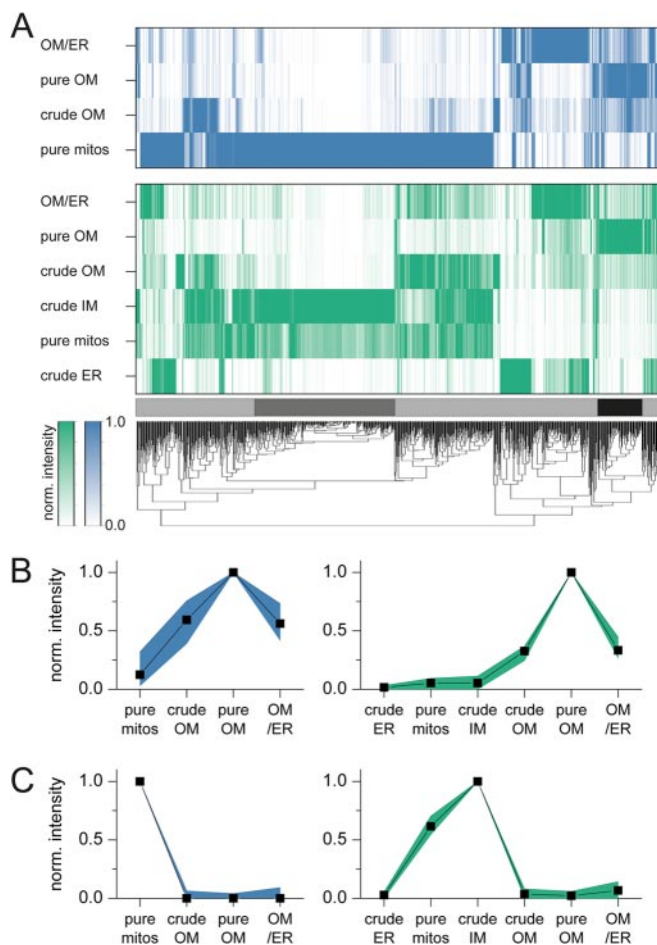


FIG. 3. **Defining the mitochondrial OM proteome by means of protein profiling and cluster analysis.** A, 1062 proteins were quantitatively followed through four and six distinct subcellular fractions obtained during the purification of OMs in experiments 1 and 2, respectively. Abundance profiles of proteins were calculated and subjected to hierarchical clustering, allowing us to define a cluster of putative OM (black bar) and IM (dark gray bar) proteins. B, C, normalized average abundance profiles of all proteins of the OM and IM clusters. The median (black line) and middle 50% (shaded area) are indicated.

Notably, the OM and IM proteomes comprise only 4% and 13% of all the proteins identified in this study. Moreover, these constituents represent only a minor fraction of all the proteins identified in highly purified OM and crude IM fractions via high-performance LC/MS (see Table I).

In summary, the data presented here underscore the effectiveness of our quantitative proteomics strategy for gaining comprehensive and accurate information about submitochondrial proteomes.

(COX 4, CYT C1), and the ER (BiP, GPI16) were measured via label-free quantitative mass spectrometry, normalized, and plotted against the corresponding subcellular fractions obtained during OM preparations in experiments 1 and 2. COX 4, cytochrome oxidase subunit 4; CYT C1, cytochrome C1; BiP, ER-localized Hsp70-like chaperone.

TABLE II
High-confidence *T. brucei* mitochondrial OM proteins of unknown function

Accession number	Name	Predicted domains	MW, molecular weight	TMD, transmembrane domain
Tb09.160.1070	POMP1		41.5	1
Tb09.160.1310 ^a	POMP2		66.5	1
Tb09.160.1330	POMP3		41.2	2
Tb09.160.4440	POMP4		30.5	–
Tb09.211.0760 ^a	POMP5		28.7	–
Tb09.211.1940 ^a	POMP6		19	–
Tb09.211.3500 ^a	POMP7		58.2	–
Tb09.211.3990 ^a	POMP8		27.9	4
Tb11.01.3290 ^a	POMP9	TPR, HCP repeats	69	–
Tb11.01.4740 ^a	POMP10		62.2	1
Tb11.02.0180 ^a	POMP11		41.6	6
Tb11.02.0350 ^a	POMP12		53	–
Tb11.02.0600 ^a	POMP13	WD40 repeat-like	39.6	1
Tb11.02.3310 ^a	POMP14		13.6	–
Tb11.02.5105 ^a	POMP15		15	–
Tb11.02.5660 ^a	POMP16	Armadillo-type fold	46.2	1
Tb11.52.0006	POMP17	Prefoldin and myosin superfamily	139	–
Tb927.1.3800 ^a	POMP18	OsmC-like	19.9	–
Tb927.10.510 ^a	POMP19		37.1	–
Tb927.10.9140 ^a	POMP20	FAD/nucleotide binding	71.9	–
Tb927.10.11030 ^a	POMP21		11.3	–
Tb927.2.5530, ^a Tb927.2.5610 ^a	POMP22		162.5	–
Tb927.3.1080 ^a	POMP23	DUF1295	28.4	4
Tb927.3.3130 ^a	POMP24		178.1	1
Tb927.3.3520 ^a	POMP25	SAM motif	47.6	–
Tb927.3.4640 ^a	POMP26	DUF125	30.4	4
Tb927.4.1540	POMP27		55.2	1
Tb927.4.1590 ^a	POMP28		39.7	–
Tb927.4.1670	POMP29	Cytochrome b5-like, heme-binding	17.4	–
Tb927.6.1550	POMP30	LRR (RNI-like superfamily)	38.9	1
Tb927.6.3680 ^a	POMP31		27.9	3
Tb927.6.4180	POMP32	FUN	16.3	2
Tb927.7.2960 ^a	POMP33	Ca-binding EF-hand	51.6	–
Tb927.7.4890 ^a	POMP34		92.7	1
Tb927.7.4980 ^a	POMP35	Zn-finger	43.4	1
Tb927.7.5470 ^a	POMP36	Ca-binding EF-hand	74.7	1
Tb927.7.7210 ^a	POMP37	CHP	77.5	–
Tb927.8.1470 ^a	POMP38		62.3	–
Tb927.8.2070, ^a Tb927.8.2260 ^a	POMP39		21.8	–
Tb927.8.2270, ^a Tb927.8.2280 ^a				
Tb927.8.4380 ^a	POMP40		11.9	1
Tb927.8.5130 ^a	POMP41		62.3	–
Tb927.8.6080	POMP42		38.1	–

^a Conserved in trypanosomatids only.

Verification of OM Localization of Seven POMPs—Despite the virtual absence of obvious contaminants, we decided to verify the localization of seven POMP. Protease treatment is the standard assay to establish the intramitochondrial localization of a protein, and the only proteins sensitive to proteolytic cleavage in intact mitochondria are OM proteins. Transgenic cell lines were produced expressing c-MYC-tagged versions of the proteins, and mitochondria were isolated under isotonic conditions, which retains the integrity of the OM (28). Isolated organelles were incubated with proteinase K, which is expected to selectively cleave OM proteins and leave proteins of the other submitochondrial fractions intact. How-

ever, the protease shaving assay is informative only when performed with mitochondria that have an intact OM. The intactness of the OM was assayed using immunoblots that determined the ratio of matrix-localized heat shock protein 70 (mHSP70) to the intermembrane space protein cytochrome c (CYT C). Mitoplasts are devoid of CYT C because their OM is disrupted (Fig 4A, first lane), which results in a high mHSP70/CYT C ratio. In intact mitochondria, however, CYT C remains in the intermembrane space, yielding a much lower mHSP70/CYT C ratio. The graph in Fig. 4A shows that isolated mitochondria from all the cell lines used for the protease shaving experiments have a low mHSP70/CYT C ratio relative to mi-

TABLE III
High-confidence *T. brucei* mitochondrial OM proteins sorted according to functional group

Accession number	Name/description	MW, molecular weight	TMD, transmembrane domain
Transport (ions and metabolites)			
Tb11.01.2550	VDAC-like	30.9	–
Tb11.03.0540	ABC transporter, putative	76.3	6
Tb927.1.4420	ABC transporter, putative	104.7	–
Tb927.2.2510, Tb927.2.2520	VDAC	29.2	–
Tb927.2.5410	ABC-transporter, putative; multidrug resistance protein	142.7	1
Tb927.4.1610	VDAC-like	39.6	–
Tb927.8.1850	MICU1, mitochondrial calcium-uptake 1	45.7	–
Transport (protein)			
Tb09.211.1240	ATOM	38.3	–
Tb927.3.4380	SAM50	53.6	–
Tb927.7.5700	pATOM36	36	–
Tb927.8.6600	SAM35, putative	35.6	–
Signaling/G-proteins			
Tb09.211.2330	Small GTPase/GTP-binding protein, putative	23.8	–
Tb11.01.5660	Cyclin 2, G1 cyclin	24.3	–
Tb11.01.6890	Small GTPase/ras-related protein rab-2a, putative	23.5	–
Tb927.10.1070	Cell division protein kinase 2 homolog 1	39.6	–
Tb927.7.7170	CYC2-like cyclin, putative	79	–
Tb927.8.560	GEM1, putative	64.6	1
Tb927.8.4610	Small GTP binding protein Rab1 (Trab1)	24	–
Lipid metabolism			
Tb09.160.2770	Fatty acyl CoA synthetase 1	79	–
Tb09.160.2840	Fatty acyl CoA synthetase 4	77.9	–
Tb09.211.4600	Short-chain dehydrogenase, putative	51.1	–
Tb11.01.1780	Short-chain dehydrogenase, putative	34	2
Tb927.3.1840	3-oxo-5-alpha-steroid 4-dehydrogenase, putative	33.4	4
Tb927.6.3050	Fatty aldehyde dehydrogenase family, putative	59.7	–
Tb927.6.3630	Sphingosine 1-phosphate lyase, putative	59.5	–
Tb927.6.710	Dephospho-CoA kinase, putative	26.9	1
Tb927.8.7120	Squalene synthase, putative	51.5	–
Protein folding/turnover			
Tb09.211.0680	CAAX prenyl protease 1, putative	48.9	5
Tb11.01.4060	Ubiquitin carboxyl-terminal hydrolase, putative	89.1	–
Tb927.7.540	Chaperone protein DNAj, putative	50.7	–
Tb927.7.990	Chaperone protein DNAj, putative	86.6	–
Redox enzymes			
Tb09.211.4110	NADPH-cytochrome p450 reductase, putative	76.9	1
Tb11.01.1690	NIDM subunit of complex I	30.3	–
Tb11.01.5225	Cytochrome b5, putative	12.9	1
Tb927.2.5180	Aldo-keto reductase, putative	38.3	–
Morphology			
Tb927.5.960	MSP-1, putative	37.2	–
Other/rest			
Tb09.160.4560	Arginine kinase	44.7	–
Tb927.5.2380	Hydrolase, alpha/beta fold family, putative	34.4	–
Tb927.6.2540	DREV methyltransferase, putative	35.9	–
Tb927.6.3510	tRNA modification enzyme, putative	59.7	1

toplasts, indicating that their OM is still intact. Fig. 4B shows that all tested POMP can be efficiently digested by proteinase K in intact mitochondria, confirming that they are *bona fide* mitochondrial OM proteins. The same immunoblots were also decorated with an antiserum against the IM mitochondrial carrier protein MCP-5 (47), which serves as a loading control. In addition to the seven POMP, we also verified the OM localization of the trypanosomal SAM35 orthologue.

Relative Abundance of Trypanosomal OM Proteins—The OM proteome was further assessed by calculating log₁₀ intensity plots of all proteins uniformly identified in pure mitosomes in order to provide an estimate of their relative abundance. The abundance distribution of the 982 proteins, including 69 OM proteins, was found to span approximately 5 orders of magnitude (Fig. 5A and supplemental Table S4). The remaining 13 putative OM proteins, including the trypano-

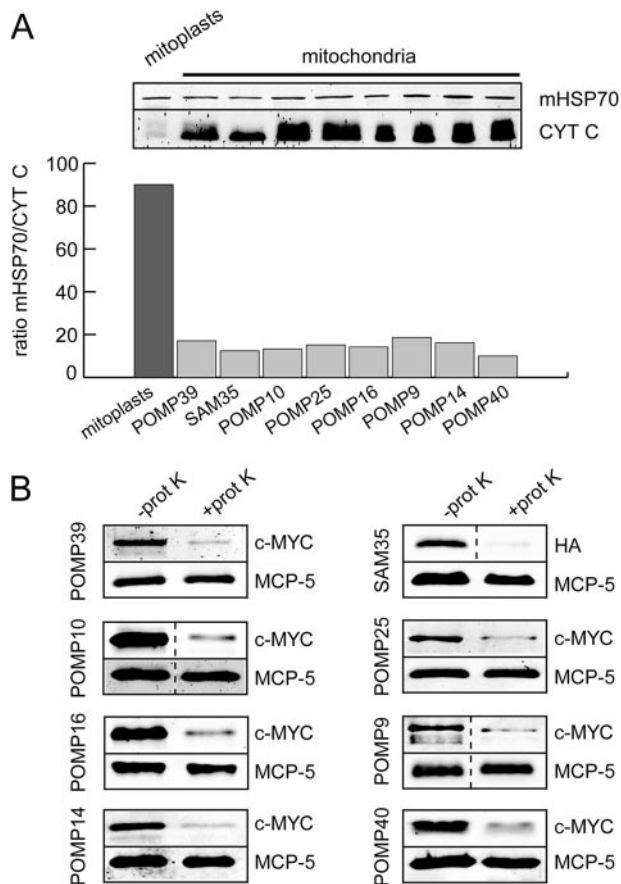


FIG. 4. Validation of the localization of selected OM proteins by protease treatment of intact mitochondria. *A*, (upper panel) 10 μ g each of hypotonically isolated mitoplasts from wild-type cells and isotopically isolated mitochondria (20) containing the indicated c-MYC-tagged proteins were analyzed via immunoblots using antibodies directed against mHSP70 and CYT C, respectively. The graph below presents quantification of the mHSP70/CYT C ratio for the samples shown above. *B*, the same mitochondria (25 μ g each) that are shown in *A* were left untreated or were incubated with proteinase K for 15 min on ice. POMP14, -16, -25, -39, and -40 and SAM35 were treated with 50 μ g/ml of proteinase K, whereas POMP9 and -10 received 250 μ g/ml of proteinase K. Subsequently, samples were analyzed via immunoblotting using antisera directed against the c-MYC and HA epitopes. Antibodies directed against the IM protein MCP-5 were used as a loading control.

somal SAM35 orthologue, could not be detected in pure mitoplast fractions and are therefore not included in the intensity plots. However, based on the intensity values observed in pure OM fractions, the abundance of SAM35 is estimated to be 2 orders of magnitude lower than that of SAM50. These findings underscore the need for effective suborganellar fractionation to detect even minor, but functionally important, OM constituents. Among the four known OM proteins, SAM50 exhibits the lowest abundance, whereas VDAC represents the most abundant OM constituent. Interestingly, ATOM was found to be a mitochondrial OM protein of high abundance, and pATOM36 (23) is less abundant by approximately a factor of

10 (Fig. 5B). Among the seven new OM constituents whose localization was confirmed by protease treatment (see Fig. 4), POMP10 was found to have an abundance similar to that of ATOM, and POMP25 was found to be approximately 3 orders of magnitude less abundant than POMP10 (Fig. 5C).

The Trypanosomal OM Proteome Contains Mainly Unstudied Proteins—Two proteomic studies characterizing the total and membrane proteomes of the *T. brucei* mitochondrion have been published before (16, 17). However, the previously detected 662 proteins that could be localized to mitochondria with high and medium confidence included only 14 proteins (17%) that are present in our OM proteome. This is consistent with the fact that the previous proteomic analyses were performed with hypotonically isolated organelles that are depleted in the OM (20). Of all experimentally identified OM proteins, an estimated 55 have not previously been associated with the mitochondrion and, to our knowledge, have not been studied before.

A significant fraction of the OM proteins (30 proteins, 36.6% of the OM proteome) contain at least one predicted transmembrane helix. The relatively large proportion of OM proteins that lack apparent transmembrane helices is expected, because the OM purification protocol in our study does not select for integral membrane proteins and detects peripheral membrane proteins as well. Moreover, some OM proteins are beta-barrel membrane proteins, which lack classical membrane spanning domains.

Conserved Features of Mitochondrial OM Proteomes—The mitochondrial OM proteome has been analyzed in two fungal and one plant species. In *Neurospora crassa*, 30 proteins were localized to the mitochondrial OM (estimated coverage of 65%) (25). Orthologues of virtually all of these proteins were also found in the much larger mitochondrial OM proteome of *S. cerevisiae*, which consists of 82 different proteins (estimated coverage of 85%) (24). In the plant *A. thaliana*, 42 proteins were assigned to the OM (estimated coverage of 88%) (26). The mitochondrial OM proteome of *T. brucei* as determined in this study consists of 82 different proteins. Fungi, plants, and trypanosomes belong to three different eukaryotic supergroups (48). Defining the OM proteomes from these species therefore allows one to identify a set of proteins that are likely found in the mitochondrial OM of all eukaryotes (Table IV). These universally conserved OM proteins are VDAC, Tom40, SAM50, SAM35, and the GEM1 GTPase. VDAC is the most abundant OM protein in all species investigated and is responsible for metabolite transport across the OM. Interestingly, all systems appear to have several different VDAC isoforms. In *T. brucei*, initially only one VDAC was found (21), but more elaborate bioinformatic analysis revealed the presence of two additional highly diverged VDAC-like proteins whose functions are unknown (49). Tom40 is the general protein import channel. Also, the *T. brucei* mitochondrial OM contains a protein that shows limited similarity to Tom40 (7). The protein was termed ATOM and is unique in that it also is

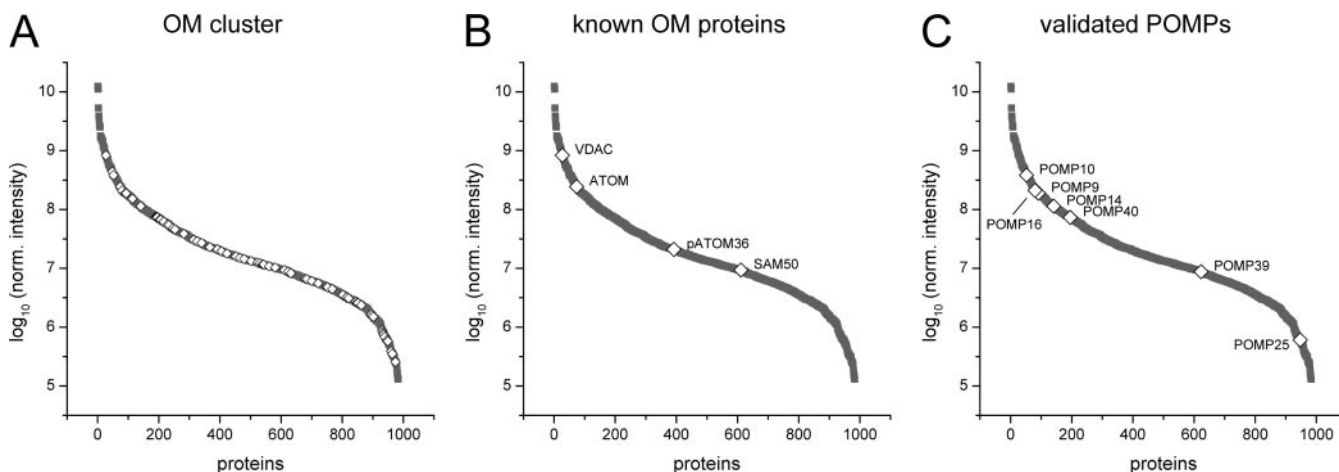


FIG. 5. **Abundance of trypanosomal OM proteins.** Log₁₀ intensity plots were calculated based on normalized intensity values of proteins identified in pure mitos fractions of experiments 1 and 2. The relative abundance of 982 proteins is shown. OM proteins are denoted by a rhombus. *A*, the abundance distribution of 69 OM proteins identified in pure mitos fractions covers nearly 4 orders of magnitude. *B*, the relative abundance levels of the four known OM proteins are shown. VDAC is the most abundant OM protein, and SAM50 is ~100 times less abundant than VDAC. *C*, abundance distribution of all seven validated POMPs.

TABLE IV
Comparison of mitochondrial OM proteomes from *T. brucei*, *S. cerevisiae*, and *A. thaliana*

Protein	<i>T. brucei</i>	<i>S. cerevisiae</i>	<i>A. thaliana</i>
VDAC, VDAC-like proteins	3	2	4
SAM50	1	1	2
SAM35	1	1	1
TOM40 ^a	(1)	1	1
GEM1 (Miro GTPase)	1	1	1
Small GTPase/GTP binding protein/G-protein, rab subfamily ^b	3	5	–
Fatty acyl CoA synthetase 4	1	1	–
Fatty aldehyde dehydrogenase	1	1	–
CAAX prenyl protease 1 (metallo-peptidase)	1	1	–
MSP-1	1	1	–
Hypothetical protein, conserved—FUN domain	1	1	–
Squalene synthase	1	1	–
NADPH-cytochrome p450 reductase	1	1	–
NADH-cytochrome b5 reductase	–	1	1
Aminoacyl-tRNA hydrolase	–	1	1

^a ATOM of *T. brucei* is similar to both the bacterial Omp85-like protein family and eukaryotic Tom40.

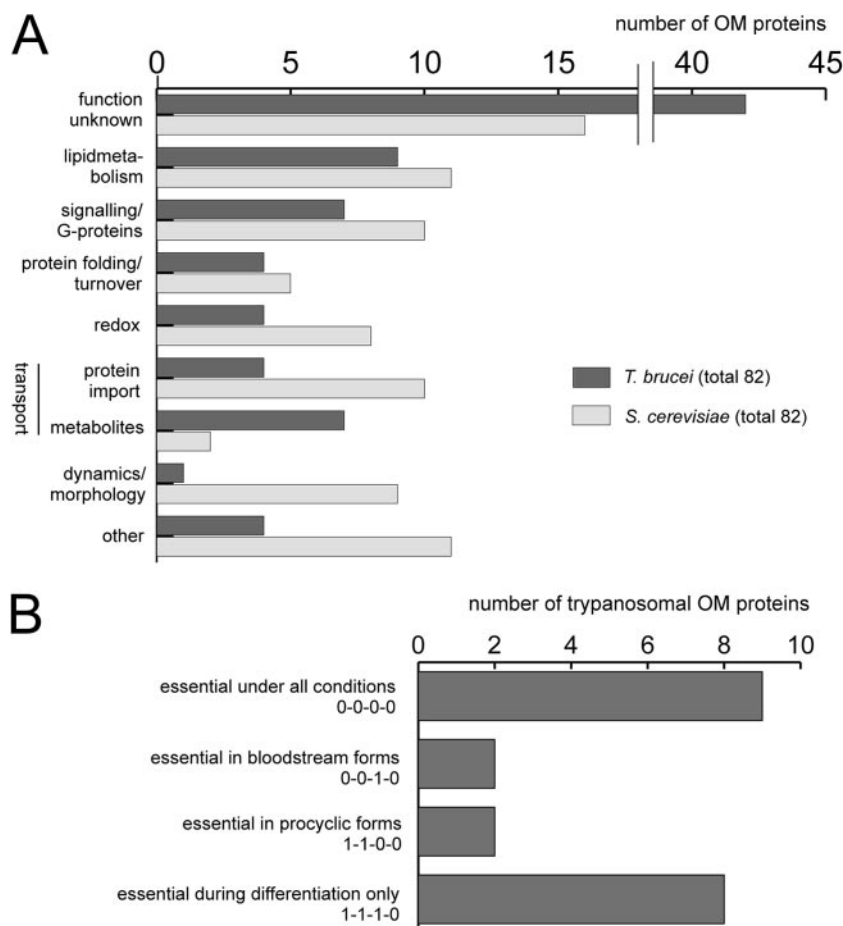
^b The putative small GTPases identified in *T. brucei* all belong to the rab subfamily but cannot be categorized further with adequate levels of confidence.

similar to the bacterial Omp85-like protein family (6, 8, 9). SAM50 and SAM35 are components of the highly conserved beta-barrel protein insertion machinery (50). GEM1 appears to be involved in the regulation of ER/mitochondria contact sites and mitochondrial morphology, respectively (40). Its universal presence in the OM proteomes suggests that ER/mitochondria contact sites are of importance in all eukaryotes.

The sizes of the OM proteomes of unicellular *T. brucei* and *S. cerevisiae* are identical, and a global comparison reveals many shared features. The fractions of OM proteins attributed to the functional groups of “lipid metabolism,” “signaling/G-proteins,” and “protein folding/turnover” are of similar size in both organisms. Within the group of “lipid metabolism,” fatty acyl CoA synthetase subunit 4, fatty aldehyde

dehydrogenase, and squalene synthase are found in both OM proteomes. In the group of “signaling/G-proteins,” a number of small GTPases of the rab subfamily are present in the OM proteomes of both *T. brucei* and yeast. In the “protein folding/turnover” group, the CAAX prenyl protease is detected in both proteomes. Moreover, components of the ubiquitin protein degradation system, although not the same ones, are found in the OM of both species. All in all, we find that the orthologues of 17 different OM proteins of *T. brucei*, corresponding to 20.7% of the OM proteome, are also present in the yeast mitochondrial OM (Table IV). Except for VDAC, GEM1, and the components of the protein import system, the function of these conserved OM proteins is unknown.

FIG. 6. Comparison of the OM proteomes of *T. brucei* and *S. cerevisiae* according to functional groups. A, histograms depicting the number of trypanosomal and yeast mitochondrial OM proteins that were classified into the functional groups indicated in Tables II and III. B, histogram depicting the number of mitochondrial OM proteins of *T. brucei* that, according to a global RNAi analysis by Alford *et al.* (27), are essential (i) for growth under all tested conditions (0-0-0-0), (ii) for growth of either bloodstream (0-0-1-0) or procyclic forms (1-1-0-0) only, or (iii) for differentiation of bloodstream to procyclic forms only (1-1-1-0). The binary code in parentheses is described in Ref. 27. For details, see supplemental Table S5.



Unique Features of the OM Proteome of *T. brucei*—Comparative analysis of the trypanosomal and yeast mitochondrial OM proteomes also uncovers striking differences. Proteins categorized in the functional groups of “protein import” and “dynamics/morphology” are strongly underrepresented in the mitochondrial OM proteome of *T. brucei*, whereas the proteins associated with metabolite transport are overrepresented (Fig. 6A). The latter fact is mainly due to the presence of three ABC transporters that are not found in the OM proteome of yeast.

The paucity of recognizable protein import factors in the trypanosomal OM proteome is in line with the fact that even the normally conserved protein import pore of the OM (6) and a receptor-like component of the protein import system (23) are highly diverged in trypanosomes. The absence of orthologues of the other protein import factors is therefore not surprising. However, the number and kinds of proteins that need to be imported into the trypanosomatid mitochondrion are comparable to those in other unicellular organisms, indicating that the protein import system, although different, will be similar in terms of complexity to those in other eukaryotes. We therefore expect that some of the POMPs are trypanosomatid-specific components of the mitochondrial protein import system.

The virtual absence of proteins that belong to the group “mitochondrial dynamics/morphology” in the *T. brucei* OM proteome is surprising because the main components of the mitochondrial fission and fusion machineries are conserved (51). However, it is in line with the fact that mitochondrial dynamics in trypanosomatids shows unique features.

Ablation of *POMP9*, *-14*, and *-40* Affects Mitochondrial Morphology—The single mitochondrion of *T. brucei* divides in two only during cytokinesis to allow its transmission to the daughter cells (52, 53). In trypanosomatids, mitochondrial fusion has never been observed, and mitochondrial fission must be coordinated with the cell cycle. As in other systems, fission requires the dynamin-like protein DLP1, which is the single member of the dynamin protein family found in trypanosomatids (53, 54). Moreover, ablation of DLP1 in *T. brucei* caused the accumulation of cells that are blocked in cytokinesis, suggesting that mitochondrial division acts as a checkpoint for cell division (53). Maintaining a single mitochondrion at all times, both the regulated fission prior to cytokinesis and the morphology change during the life cycle are expected to require as yet unknown factors associated with the trypanosomal mitochondrial OM. We therefore expect that some of the POMPs will be such factors. As a first test for this prediction, we prepared inducible RNAi cells directed against

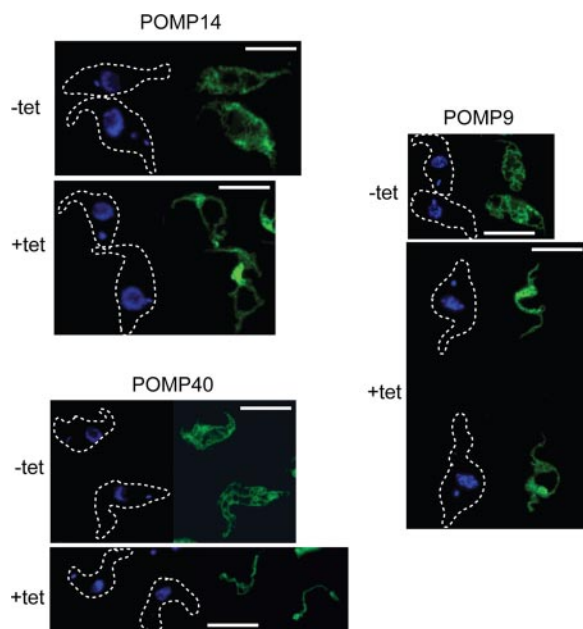


FIG. 7. Ablation of POMP9, -14, and -40 affects mitochondrial morphology. Procyclic 29–13 cell lines allowing tetracycline inducible ablation of POMP9, POMP14, and POMP40 were tested for alterations of mitochondrial morphology. Left-hand panels: uninduced (-tet) and induced (+tet) cells were stained for DNA using 4'-6-diamidino-phenylindole (blue). The outlines of the cells have been traced in the phase contrast channel and are projected onto the stained pictures. The mitochondrion from uninduced (-tet) and induced (+tet) RNAi cell lines was visualized using anti-ATOM antiserum (green). The percentages of induced cells showing an altered mitochondrial morphology were 96%, 96%, and 98% for POMP9, POMP14, and POMP40, respectively. Scale corresponds to 10 μm .

POMP9, POMP14, and POMP40. RNAi-mediated ablation shows that all three proteins are essential for normal growth in procyclic cells (data not shown). Mitochondrial morphology was analyzed via immunofluorescence microscopy using anti-ATOM antiserum (Fig. 7). Individual ablation of all three proteins dramatically altered the network-like mitochondrial structure in procyclic trypanosomes. The strongest phenotype was observed for the POMP40 RNAi cells. Their mitochondria collapsed from a highly branched structure to an essentially straight single tubule, reminiscent of the mitochondrial shape observed in the bloodstream form (55). The induction of RNAi causes a collapse of the network for POMP9 and POMP14, as well; however, the phenotype is less severe, and a more condensed form of the network appears to be maintained. In conclusion, we report POMP9, POMP14, and POMP40 as the first factors known to regulate mitochondrial morphology in *T. brucei*. These results illustrate the value of the OM proteome for identifying novel factors that directly or indirectly control mitochondrial morphology.

The Mitochondrial OM Proteome Contains Essential Proteins—Recently, a global high-throughput analysis was performed that mapped the fitness costs associated with the inducible RNAi-mediated ablation of mRNAs encoded by es-

entially all trypanosomal ORFs (27). The effect the RNAi has on the growth of *T. brucei* was measured under four different conditions: in procyclic forms after 3 days of induction, in the bloodstream forms 3 and 6 days after induction, and in differentiating cells.

Nine proteins from the *T. brucei* OM proteome are essential under all tested conditions, and two proteins each are essential for the bloodstream and the procyclic forms. Eight OM proteins appear to be specifically required for the differentiation of the bloodstream form to the procyclic form (Fig. 6B, supplemental Table S5). Preliminary validation experiments using individual RNAi cell lines against some OM proteins indicate that the global analysis is probably biased toward false negatives, suggesting that the number of essential OM proteins might even be higher (data not shown).

The nine proteins that are essential under all conditions are of special interest because they are required for core essential functions. Five of them—namely, ATOM, pATOM36, POMP6, POMP14, and POMP22—are specific for trypanosomatids. The function of these three POMP is not known, but the only essential function of mitochondrial OM proteins described so far is protein import. This suggests that these POMP might represent as yet unknown factors of the mitochondrial protein import machinery that are specific for trypanosomatids. Moreover, the trypanosomal mitochondrion lacks tRNA genes and therefore needs to import all of its tRNA from the cytosol (5). Mitochondrial translation was shown to be essential not only for the procyclic but also for the bloodstream form of *T. brucei* (56), indicating that the same must be true for mitochondrial tRNA import. Thus, we expect that the machinery for mitochondrial tRNA import also is encoded by POMP that encode core essential functions. It is even possible, as has been suggested for the mitochondrial IM (57, 58), that some protein import factors might also be required for tRNA import. Interestingly, of the three newly discovered factors that are required in order to maintain normal mitochondrial morphology (Fig. 7), only POMP14, and not POMP9 or POMP40, is required for core essential functions as defined by Ref. 27 (supplemental Table S5).

Concluding Remarks—*Trypanosoma brucei* is a unicellular eukaryote that causes devastating diseases in humans and animals. It has a unique evolutionary history that has resulted in a mitochondrion showing many distinct features relative to other eukaryotes. Several of these features are linked to the OM, which forms the interface between the mitochondrion and the cytosol. They include unusual protein and tRNA import systems and a unique mitochondrial shape that is highly regulated. The 82 OM proteins that were identified in our study will be a treasure trove of insight into these processes. Most of the 82 OM proteins have never been identified before, and 33 are specific for trypanosomatids. The latter are of special interest because a comparison with the yeast OM proteome reveals a strong underrepresentation of protein import factors and orthologues of proteins that regulate the

shape of the mitochondrion. This suggests that many of the trypanosomal OM proteins of unknown function recovered in the present study might be required either for protein import or for the maintenance of mitochondrial morphology. In line with the latter prediction, we used RNAi to identify three OM proteins of unknown function as the first candidate factors for the regulation of mitochondrial morphology in *T. brucei*.

Finally, it is worth noting that ATOM, pATOM36, and three POMP (6, 14, and 22) are essential for the bloodstream form of *T. brucei*. These proteins might therefore represent excellent novel drug targets, as they are specific for trypanosomatids and essential for the disease-causing form of the parasite. Studying their function not only will be of interest for basic science but also is likely to provide novel targets for future drug development.

Acknowledgments—We thank J. Bangs (University of Wisconsin-Madison), A. Jardim (McGill University), R. Jensen (John Hopkins School of Medicine), K. Matthews (University of Edinburgh), T. Seebeck (University of Bern), and F. Voncken (University of Hull) for antisera; S. Vainauskas, J. Bangs, and A. Menon (Weill Cornell Medical College) for the gift of the GPI16:HA construct; and M. Schmid and A. Albisetti for their help with the proteinase K shaving experiments.

* M.N. gratefully acknowledges a personal fellowship of the Peter und Traudl Engelhorn foundation. Research in the groups of C.M. and B.W. was funded by the Deutsche Forschungsgemeinschaft and the Excellence Initiative of the German Federal & State Governments (EXC 294 BIOSS Centre for Biological Signaling Studies). Research in the lab of A.S. was supported by Grant No. 138355 from the Swiss National Foundation.

§ This article contains [supplemental material](#).

‡ To whom correspondence should be addressed: André Schneider, Tel.: +41 31 631 4253, Fax: +41 31 631 48 87, E-mail: andre.schneider@ibc.unibe.ch; or Bettina Warscheid, Tel.: +49 761 203 2690, Fax: +49 761-203-2601, E-mail: bettina.warscheid@biologie.uni-freiburg.de.

§ These authors contributed equally to this work.

REFERENCES

- Lüscher, A., Koning, H. P. d., and Mäser, P. (2007) Chemotherapeutic strategies against *Trypanosoma brucei*: drug targets vs. drug targeting. *Curr. Pharm. Des.* **13**, 555–567
- Cavalier-Smith, T. (2010) Kingdoms Protozoa and Chromista and the eozoan root of the eukaryotic tree. *Biol. Lett.* **6**, 342–345
- Lukes, J., Hashimi, H., and Ziková, A. (2005) Unexplained complexity of the mitochondrial genome and transcriptome in kinetoplastid flagellates. *Curr. Genet.* **48**, 277–299
- Stuart, K. D., Schnauffer, A., Ernst, N. L., and Panigrahi, A. K. (2005) Complex management: RNA editing in trypanosomes. *Trends Biochem. Sci.* **30**, 97–105
- Schneider, A. (2011) Mitochondrial tRNA import and its consequences for mitochondrial translation. *Ann. Rev. Biochem.* **80**, 1033–1053
- Pusnik, M., Schmidt, O., Perry, A. J., Oeljeklaus, S., Niemann, M., Warscheid, B., Lithgow, T., Meisinger, C., and Schneider, A. (2011) Mitochondrial preprotein translocase of trypanosomatids has a bacterial origin. *Curr. Biol.* **21**, 1738–1743
- Zarsky, V., Tachezy, J., and Dolezal, P. (2012) Tom40 is likely common to all mitochondria. *Curr. Biol.* **22**, R479–R481
- Pusnik, M., Schmidt, O., Perry, A. J., Oeljeklaus, S., Niemann, M., Warscheid, B., Meisinger, C., Lithgow, T., and Schneider, A. (2012) Response to Zarsky et al. *Curr. Biol.* **22**, R481–R482
- Harsman, A., Niemann, M., Pusnik, M., Schmidt, O., Burmann, B. M., Hiller, S., Meisinger, C., Schneider, A., and Wagner, R. (2012) Bacterial origin of a mitochondrial outer membrane protein translocase: new perspectives from comparative single channel electrophysiology. *J. Biol. Chem.* **287**, 31437–31445
- Simpson, L., and Kretzer, F. (1997) The mitochondrion in dividing *Leishmania tarentolae* cells is symmetric and circular and becomes a single asymmetric tubule in non-dividing cells due to division of the kinetoplast portion. *Mol. Biochem. Parasitol.* **87**, 71–78
- Tyler, K. M., Matthews, K. R., and Gull, K. (1997) The bloodstream differentiation-division of *Trypanosoma brucei* studied using mitochondrial markers. *Proc. R. Soc. Lond.* **264**, 1481–1490
- Matthews, K. R. (2005) The developmental cell biology of *Trypanosoma brucei*. *J. Cell Sci.* **118**, 283–290
- Priest, J. W., and Hajduk, S. L. (1994) Developmental regulation of mitochondrial biogenesis in *Trypanosoma brucei*. *J. Bioenerg. Biomemb.* **26**, 179–191
- Schneider, A. (2001) Unique aspects of mitochondrial biogenesis in trypanosomatids. *Int. J. Parasitol.* **31**, 1403–1415
- Besteiro, S., Barrett, M. P., Riviere, L., and Bringaud, F. (2005) Energy generation in insect stages of *Trypanosoma brucei*: metabolism in flux. *Trends Parasitol.* **21**, 185–191
- Panigrahi, A. K., Ogata, Y., Ziková, A., Anupama, A., Dalley, R. A., Acestor, N., Myler, P. J., and Stuart, K. D. (2009) A comprehensive analysis of *Trypanosoma brucei* mitochondrial proteome. *Proteomics* **9**, 434–450
- Acestor, N., Panigrahi, A. K., Ogata, Y., Anupama, A., and Stuart, K. D. (2009) Protein composition of *Trypanosoma brucei* mitochondrial membranes. *Proteomics* **9**, 5497–5508
- Acestor, N., Ziková, A., Dalley, R. A., Anupama, A., Panigrahi, A. K., and Stuart, K. D. (2011) *Trypanosoma brucei* mitochondrial respiratome: composition and organization in procyclic form. *Mol. Cell. Proteomics* **10**, M110.006908
- Ziková, A., Panigrahi, A. K., Dalley, R. A., Acestor, N., Anupama, A., Ogata, Y., Myler, P. J., and Stuart, K. (2008) *Trypanosoma brucei* mitochondrial ribosomes: affinity purification and component identification by mass spectrometry. *Mol. Cell. Proteomics* **7**, 1286–1296
- Schneider, A., Charrière, F., Pusnik, M., and Horn, E. K. (2007) Isolation of mitochondria from procyclic *Trypanosoma brucei*. *Methods Mol. Biol.* **372**, 67–80
- Pusnik, M., Charrière, F., Mäser, P., Waller, R. F., Dagley, M. J., Lithgow, T., and Schneider, A. (2009) The single mitochondrial porin of *Trypanosoma brucei* is the main metabolite transporter in the outer mitochondrial membrane. *Mol. Biol. Evol.* **26**, 671–680
- Sharma, S., Singha, U. K., and Chaudhuri, M. (2010) Role of Tob55 on mitochondrial protein biogenesis in *Trypanosoma brucei*. *Mol. Biochem. Parasitol.* **174**, 89–100
- Pusnik, M., Mani, J., Schmid, O., Niemann, M., Oeljeklaus, S., Schnarwiler, F., Warscheid, B., Lithgow, T., Meisinger, C., and Schneider, A. (2012) An essential novel component of the non-canonical mitochondrial outer membrane protein import system of trypanosomatids. *Mol. Biol. Cell* **23**, 3420–3428
- Zahedi, R. P., Sickmann, A., Boehm, A. M., Winkler, C., Zufall, N., Schönfisch, B., Guiard, B., Pfanner, N., and Meisinger, C. (2006) Proteomic analysis of the yeast mitochondrial outer membrane reveals accumulation of a subclass of preproteins. *Mol. Biol. Cell* **17**, 1436–1450
- Schmitt, S., Prokisch, H., Schlunck, T., Camp, D. G., Ahting, U., Waizenegger, T., Scharfe, C., Meitinger, T., Imhof, A., Neupert, W., Oefner, P. J., and Rapaport, D. (2006) Proteome analysis of mitochondrial outer membrane from *Neurospora crassa*. *Proteomics* **6**, 72–80
- Duncan, O., Taylor, N. L., Carrie, C., Eubel, H., Kubiszewski-Jakubiak, S., Zhang, B., Narsai, R., Millar, A. H., and Whelan, J. (2011) Multiple lines of evidence localize signaling, morphology, and lipid biosynthesis machinery to the mitochondrial outer membrane of *Arabidopsis*. *Plant Physiol.* **157**, 1093–1113
- Alsford, S., Turner, D. J., Obado, S. O., Sanchez-Flores, A., Glover, L., Berriman, M., Hertz-Fowler, C., and Horn, D. (2011) High-throughput phenotyping using parallel sequencing of RNA interference targets in the African trypanosome. *Genome Res.* **21**, 915–924
- Hauser, R., Pypaert, M., Häusler, T., Horn, E. K., and Schneider, A. (1996) In vitro import of proteins into mitochondria of *Trypanosoma brucei* and *Leishmania tarentolae*. *J. Cell Sci.* **109**, 517–523
- Alconada, A., Gärtner, F., Hönlinger, A., Kübrich, M., and Pfanner, N. (1995)

- Mitochondrial receptor complex from *Neurospora crassa* and *Saccharomyces cerevisiae*. *Methods Enzymol.* **260**, 263–286
30. Mayer, A., Driessen, A., Neupert, W., and Lill, R. (1995) Purified and protein-loaded mitochondrial outer membrane vesicles for functional analysis of preprotein transport. *Methods Enzymol.* **260**, 252–263
 31. Wessel, D., and Fugge, U. I. (1984) A method for the quantitative recovery of protein in dilute solution in the presence of detergents and lipids. *Anal. Biochem.* **138**, 141–143
 32. Cox, J., and Mann, M. (2008) MaxQuant enables high peptide identification rates, individualized p.p.b.-range mass accuracies and proteome-wide protein quantification. *Nat. Biotechnol.* **26**, 1367–1372
 33. Cox, J., Neuhauser, N., Michalski, A., Scheltema, R. A., Olsen, J. V., and Mann, M. (2011) Andromeda: a peptide search engine integrated into the MaxQuant environment. *J. Proteome Res.* **10**, 1794–1805
 34. Oberholzer, M., Morand, S., Kunz, S., and Seebeck, T. (2005) A vector series for rapid PCR-mediated C-terminal in situ tagging of *Trypanosoma brucei* genes. *Mol. Biochem. Parasitol.* **145**, 117–120
 35. Wirtz, E., Leal, S., Ochatt, C., and Cross, G. A. (1999) A tightly regulated inducible expression system for conditional gene knock-outs and dominant-negative genetics in *Trypanosoma brucei*. *Mol. Biochem. Parasitol.* **99**, 89–101
 36. Bochud-Allemann, N., and Schneider, A. (2002) Mitochondrial substrate level phosphorylation is essential for growth of procyclic *Trypanosoma brucei*. *J. Biol. Chem.* **277**, 32849–32854
 37. Sherwin, T., Schneider, A., Sasse, R., Seebeck, T., and Gull, K. (1987) Distinct localization and cell cycle dependence of COOH terminally tyrosinolated α -tubulin in the microtubules of *Trypanosoma brucei*. *J. Cell Biol.* **104**, 439–445
 38. Smith, T. K., and Butikofer, P. (2010) Lipid metabolism in *Trypanosoma brucei*. *Mol. Biochem. Parasitol.* **172**, 66–79
 39. Parsons, D. F., Williams, G. R., and Chance, B. (1966) Characteristics of isolated and purified preparations of the outer and inner membranes of mitochondria. *Ann. N.Y. Acad. Sci.* **137**, 643–666
 40. Michel, A. H., and Kornmann, B. (2012) The ERMES complex and ER-mitochondria connections. *Biochem. Soc. Trans.* **40**, 445–450
 41. Andersen, J. S., Christopher, J., Wilkinson, J., Mayor, T., Mortensen, P., Nigg, E. A., and Mann, M. (2003) Proteomic characterization of the human centrosome by protein correlation profiling. *Nature* **426**, 570–574
 42. Foster, L. J., Hoog, C. L. d., Zhang, Y., Zhang, Y., Xie, X., Moohta, V. K., and Mann, M. (2006) A mammalian organelle map by protein correlation profiling. *Cell* **125**, 187–199
 43. Wiese, S., Gronemeyer, T., Ofman, R., Kunz, M., Grou, C. P., Almeida, J. A., Eisenacher, M., Stephan, C., Hayen, H., Schollenberger, L., Korosec, T., Waterham, H. R., Schliebs, W., Erdmann, R., Berger, J., Meyer, H. E., Just, W., Azevedo, J. E., Wanders, R. J. A., and Warscheid, B. (2007) Proteomics characterization of mouse kidney peroxisomes by tandem mass spectrometry and protein correlation profiling. *Mol. Cell. Proteomics* **6**, 2045–2057
 44. Perocchi, F., Gohil, V. M., Girgis, H. S., Bao, X. R., McCombs, J. E., Palmer, A. E., and Mootha, V. K. (2010) MICU1 encodes a mitochondrial EF hand protein required for Ca²⁺ uptake. *Nature* **467**, 291–296
 45. Stefani, D. D., Raffaello, A., Teardo, E., Szabò, I., and Rizzuto, R. (2011) A forty-kilodalton protein of the inner membrane is the mitochondrial calcium uniporter. *Nature* **476**, 336–340
 46. Baughman, J. M., Perocchi, F., Girgis, H. S., Plovanich, M., Belcher-Timme, C. A., Sancak, Y., Bao, X. R., Strittmatter, L., Goldberger, O., Bogorad, R. L., Kotliansky, V., and Mootha, V. K. (2011) Integrative genomics identifies MCU as an essential component of the mitochondrial calcium uniporter. *Nature* **476**, 341–345
 47. Colasante, C., Diaz, P. P., Clayton, C., and Voncken, F. (2009) Mitochondrial carrier family inventory of *Trypanosoma brucei brucei*: Identification, expression and subcellular localisation. *Mol. Biochem. Parasitol.* **167**, 104–117
 48. Dacks, J. B., Walker, G., and Field, M. C. (2008) Implications of the new eukaryotic systematics for parasitologists. *Parasitol. Int.* **57**, 97–104
 49. Flinner, N., Schleiff, E., and Mirus, O. (2012) Identification of two voltage-dependent anion channel-like protein sequences conserved in Kinoplastida. *Biol. Lett.* **8**, 446–449
 50. Schmidt, O., Pfanner, N., and Meisinger, C. (2010) Mitochondrial protein import: from proteomics to functional mechanisms. *Nat. Rev. Mol. Cell Biol.* **11**, 655–667
 51. Westermann, B. (2010) Mitochondrial fusion and fission in cell life and death. *Nat. Rev. Mol. Cell Biol.* **11**, 872–884
 52. Crausaz-Esseiva, A., Chanez, A.-L., Bochud-Allemann, N., Martinou, J. C., Hemphill, A., and Schneider, A. (2004) Temporal dissection of Bax-induced events leading to fission of the single mitochondrion in *Trypanosoma brucei*. *EMBO Rep.* **5**, 268–273
 53. Chanez, A.-L., Hehl, A., Engstler, M., and Schneider, A. (2006) Ablation of the single dynamin of *T. brucei* blocks mitochondrial fission and endocytosis and leads to a precise cytokinesis arrest. *J. Cell Sci.* **119**, 2968–2974
 54. Morgan, G. W., Goulding, D., and Field, M. C. (2004) The single dynamin-like protein of *Trypanosoma brucei* regulates mitochondrial division and is not required for endocytosis. *J. Biol. Chem.* **279**, 10692–10701
 55. Vassella, E., Straesser, K., and Boshart, M. (1997) A mitochondrion-specific dye for multicolour fluorescent imaging of *Trypanosoma brucei*. *Mol. Biochem. Parasitol.* **90**, 381–385
 56. Cristodero, M., Seebeck, T., and Schneider, A. (2010) Mitochondrial translation is essential in bloodstream forms of *Trypanosoma brucei*. *Mol. Microbiol.* **78**, 757–769
 57. Tschopp, F., Charrière, F., and Schneider, A. (2011) In vivo study in *Trypanosoma brucei* links mitochondrial transfer RNA import to mitochondrial protein import. *EMBO Rep.* **12**, 825–832
 58. Seidman, D., Johnson, D., Gerbasi, V., Golden, D., Orlando, R., and Hajduk, S. (2012) Mitochondrial membrane complex that contains proteins necessary for tRNA import in *Trypanosoma brucei*. *J. Biol. Chem.* **287**, 8892–8903